01 Jan 2005

# Distorted Wave Born and Three-Body Distorted Wave Born Approximation Calculations of the Fully Differential Cross Section for Electron-Impact Ionization of Nitrogen Molecules

Junfang Gao

Don H. Madison
*Missouri University of Science and Technology*, madison@mst.edu

Jerry Peacher
*Missouri University of Science and Technology*, peacher@mst.edu



## Recommended Citation

J. Gao et al., "Distorted Wave Born and Three-Body Distorted Wave Born Approximation Calculations of the Fully Differential Cross Section for Electron-Impact Ionization of Nitrogen Molecules," *Journal of Chemical Physics*, American Institute of Physics (AIP), Jan 2005.
The definitive version is available at https://doi.org/10.1063/1.2126971

# Distorted wave Born and three-body distorted wave Born approximation calculations of the fully differential cross section for electron-impact ionization of nitrogen molecules

Junfang Gao,[a] D. H. Madison, and J. L. Peacher
*Department of Physics, University of Missouri-Rolla, Rolla, Missouri 65409-0460*

(Received 29 August 2005; accepted 29 September 2005; published online 28 November 2005)

Currently there are no reliable theoretical approaches for calculating fully differential cross sections (FDCSs) for low-energy electron-impact ionization of large molecules. We have recently proposed the orientation-averaged molecular orbital (OAMO) for calculating cross sections averaged over molecular orientations. In this paper, we use the OAMO to calculate distorted wave Born approximation (DWBA) and molecular three-body distorted wave (M3DW) Born approximation FDCS for electron-impact ionization of the nitrogen molecule. Both coplanar symmetric and asymmetric FDCSs are investigated in the energy range of 35.6–400 eV. By comparing with the experimental data, we found that the M3DW is reasonably accurate in this energy range. We also found that the postcollision interaction plays a sufficiently important role and that the DWBA is not reliable. © *2005 American Institute of Physics*. [DOI: 10.1063/1.2126971]

## INTRODUCTION

Electron-impact ionization of atoms and molecules plays an important role in astrophysics, plasma physics, mass spectroscopy, and lighting industry. For the last two decades, high-energy electron ionization of molecules has been used to explore molecular structure and very valuable information about the highest occupied molecular orbital (HOMO) has been found using the $(e,2e)$ technique.[1–4] So far many molecules have been studied.[5] Whereas structure information can be determined from high-energy electron-impact ionization, information about scattering dynamics and the basic Coulomb interactions among those particles can be studied for lower impact energies. Starting in the 1970s, several experimental groups[6–15] have measured lower-energy coplanar symmetric and asymmetric fully differential cross sections (FDCSs) for different molecules and atoms. However, there is still no reliable theory to interpret these experimental data, especially for the case of low-energy electron-impact ionization of big molecules.

There have been several different theoretical models proposed since the 1970s: (1) The plane-wave impulse approximation (PWIA) developed by McCarthy and co-workers[1–3] has been very successful at high energies for studying molecular structure. (2) In 1996, Robicheaux[16] introduced an analytical method to treat electron-impact ionization of $H_2^+$ using a prolate spheroidal coordinate system. This method is a useful way to assess the experimental data and other approximations. (3) The modified additive rule (MAR) obtains molecular ionization cross sections by summing the ionization cross section for each constituent atom by incorporating atomic weighting factors. MAR was used for electron-impact ionization of $C_2H_6$ by Deutch and Becker[17] in 1998. (4) In the first Born approximation (FBA), the ejected electron is treated as a Coulomb wave whereas the incident and scattered electrons are treated as plane waves. In 2001, Champion *et al.*[18] used the FBA to study electron-impact ionization of $H_2O$. (5) Monzani *et al.*[19] reported a distorted wave Born approximation (DWBA) approach for $H_2$ in which all incoming and outgoing continuum electrons are represented as distorted waves calculated in the single-center static-exchange potential using the Schwinger variational iterative. (6) For the two-effective-center approximation for diatomic molecules, one assumes that the ejected electron is ionized from the proximity of one of the nuclei and the passive electron completely screens the other nucleus. As a result, the ejected electron interacts with only one nucleus and the projectile electron. The incident and scattered electrons are represented as plane waves. This method was used by Weck *et al.*[20] to study fast-electron-impact ionization of $H_2$ in 2001. (7) Stia *et al.*[21] introduced the molecular Brauner-Briggs-Klar (MBBK) approximation for $H_2$. (8) We have recently proposed the distorted wave impulse approximation (DWIA) using an orientation-averaged molecular orbital for electron-impact ionization of $N_2$.[22–25] Most theories are designed to treat either low-energy collisions with simple molecules or high-energy collisions with big molecules. A reliable theory for low-energy electron-impact ionization of both small and large molecules is lacking.

We will present two new theoretical models in this paper—a DWBA modeled after the corresponding calculations which have been performed for almost three decades for atoms and the molecular three-body distorted wave (M3DW) approximation which is also modeled after the atomic 3DW approximation. The difference between the DWBA and M3DW lies in the fact that the M3DW contains the postcollision interaction (PCI) between the scattered and ejected electrons to all orders of perturbation theory while the DWBA contains the PCI only to first order. The orientation-averaged molecular orbital (OAMO) which was

[a]Electronic mail: jgzm6@umr.edu

 

discussed in detail in Refs. 22 and 24 will be used to approximate the average over all molecular orientations. The DWBA and M3DW will be used to investigate FDCS for electron-impact ionization of $N_2$. The molecular orbitals (MOs) used in the calculation were generated from the Hartree-Fock code GAMESS.[26] To study the collision dynamics, we performed both coplanar symmetric and coplanar asymmetric geometry calculations. For coplanar symmetric collisions, we will compare our results with the experimental data of Hussey and Murray[9] and the data of Rioual *et al.*[8] For coplanar asymmetric collisions, we will compare with the experimental data of Avaldi *et al.*[7] a.u. are used unless noted otherwise.

## THEORY

The M3DW is very similar to the 3DW approach of Madison and co-workers.[27–29] In the M3DW approximation the $T$ matrix is given by

$$T_{fi}^{\mathrm{M3DW}} = \langle \chi_f^- \chi_e^- C_{\text{proj-eject}} | V - U_S | \phi_j^{\mathrm{OA}} \chi_i^+ \rangle, \tag{1}$$

where $\chi_i$, $\chi_f$, and $\chi_e$ are the distorted waves for the incident, scattered, and ejected electrons, respectively; $\phi_j^{\mathrm{OA}}$ is the orientation-averaged molecular wave function for the initial bound state of the molecule; $V$ is the initial-state interaction between the projectile and the neutral molecule; and $U_S$ is the spherically symmetric distorting potential which is used to calculate the initial-state distorted wave $\chi_i$. The term $C_{\text{proj-eject}}$ is the Coulomb interaction between the projectile and ejected electrons (PCI). Brauner *et al.*[30] were the first to demonstrate for electron-impact ionization of H that it was very important to include the Coulomb interaction directly in the $T$ matrix. The standard DWBA is similar to the M3DW except that the Coulomb interaction is not included in the final state wave function,

$$T_{fi}^{\mathrm{DWBA}} = \langle \chi_f^- \chi_e^- | V - U_S | \phi_j^{\mathrm{OA}} \chi_i^+ \rangle. \tag{2}$$

When the Coulomb interaction is included directly in the final-state wave function (M3DW), PCI is included to all orders of perturbation theory and when it is included only in the perturbation (DWBA), PCI is included only to first order in perturbation theory.

The molecular distorted waves are calculated using a spherically averaged distorting potential, as described in our previous works.[22–25] The Schrödinger equation for the incoming electron wave function is given by

$$\left( T + U_S + U_E - \frac{k_i^2}{2} \right) \chi_i^+(\mathbf{k}_i, \mathbf{r}) = 0, \tag{3}$$

where $T$ is the kinetic-energy operator, $U_S$ is the initial-state spherically symmetric static potential, $U_E$ is a local exchange potential, and $\mathbf{k}_i$ is the initial-state wave vector. The plus superscript on $\chi_i^+(\mathbf{k}_i, \mathbf{r})$ indicates outgoing wave bound conditions. The static potential is obtained from the Hartree-Fock charge distribution for $N_2$,

$$U_S = V_{\mathrm{nuc}}(r) + V_{\mathrm{ele}}(r), \tag{4}$$

where

$$V_{\mathrm{ele}}(r) = \left\langle \int \frac{\rho(\mathbf{r}', \mathbf{R}) d\mathbf{r}'}{|r - r'|} \right\rangle, \tag{5}$$

$$\rho(\mathbf{r}', \mathbf{R}) = \sum_{j=1}^{N} n_j |\phi_j(\mathbf{r}', \mathbf{R})|^2. \tag{6}$$

Here $\rho(\mathbf{r}', \mathbf{R})$ is the molecular charge density which depends on the internuclear vector $\mathbf{R}$ and the electronic coordinate $\mathbf{r}'$, $N$ is the number of molecular orbitals, and $n_j$ is the number of electrons in orbital $\phi_j$. We generate the molecular orbitals $\phi_j$ using the Hartree-Fock code GAMESS.[26] The brackets in Eq. (5) indicate an average over all orientation angles. For the local exchange potential, similar to the atomic case, the Furness and McCarthy[31] exchange potential is used,

$$U_E = -\tfrac{1}{2}\{(k_i^2 - U_S) - \sqrt{(k_i^2 - U_S)^2 + 2\rho_S(r)}\}, \tag{7}$$

where $\rho_S(r)$ is the spherically averaged molecular electronic charge density,

$$\rho_S(r) = \langle \rho(\mathbf{r}, \mathbf{R}) \rangle. \tag{8}$$

The radial charge density is defined such that the integral over $r$ yields the number of electrons in the molecule. The two final channel distorted waves are obtained from the Schrödinger equation similar to Eq. (3),

$$\left( T + U_I + U_E - \frac{k_{f(e)}^2}{2} \right) \chi_{f(e)}^-(\mathbf{k}_{f(e)}, \mathbf{r}) = 0. \tag{9}$$

Here $U_I$ is the spherically averaged static distorted potential for the molecular ion which is calculated using the same procedure as used for $U_S$ except the active electron is removed from the charge distribution. The minus sign in the superscript indicates incoming wave boundary conditions.

As described by Prideaux and Madison,[32] if we treat the ionization event as a three-body problem, the perturbation term can be approximated as

$$V - U_S = -\frac{1}{|r_f - r_e|} - U_{\mathrm{bound}}(r_f), \tag{10}$$

where $|r_f - r_e|$ is the distance between the two electrons and $U_{\mathrm{bound}}(r_f)$ is the spherically symmetric potential for the single active bound-state electron.

To compare with the existing experimental data which do not distinguish between different molecular orientations, the OAMO was introduced.[22–24] In Eqs. (1) and (2), the OAMO $\phi_j^{\mathrm{OA}}(\mathbf{r})$ is defined as

$$\phi_j^{\mathrm{OA}}(\mathbf{r}) = \frac{1}{4\pi} \int \phi_j(\mathbf{r}, \mathbf{R}) d\Omega_R. \tag{11}$$

Gao *et al.*[22–24] showed that using the OAMO in the evaluation of the $T$ matrix to approximate the average over all molecular orientations was valid for ionization of gerade ground states of diatomic molecules if the wave function is dominated by the $s$-basis functions and $qR \leqslant 2$ ($q$ is the momentum transferred to the ion and $R$ is the internuclear distance). For $N_2$ the ground-state wave function is dominated by $s$-basic states.

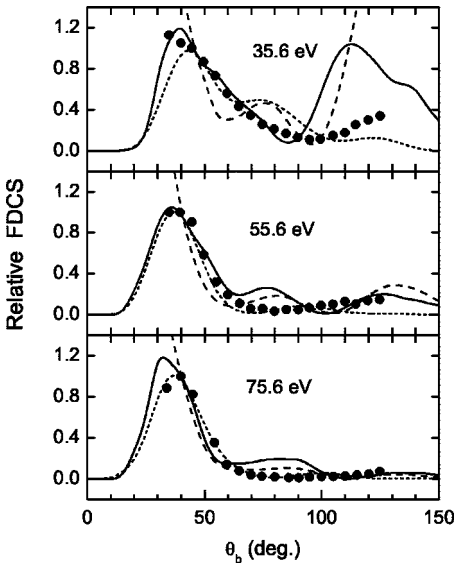


FIG. 1. Fully differential cross sections for electron-impact ionization of the $3\sigma_g$ state of $N_2$ for coplanar symmetric scattering. The energy of the incident electron is shown in each part of the figure and the horizontal axis is the angular location for the two electron detectors on the opposite sides of the beam direction. The solid lines are the M3DW results, the longer dashed lines are the DWBA results, the shorter dashed lines are the DWIA results, and the black circles are the experimental data of Hussey and Murray (Ref. 9).

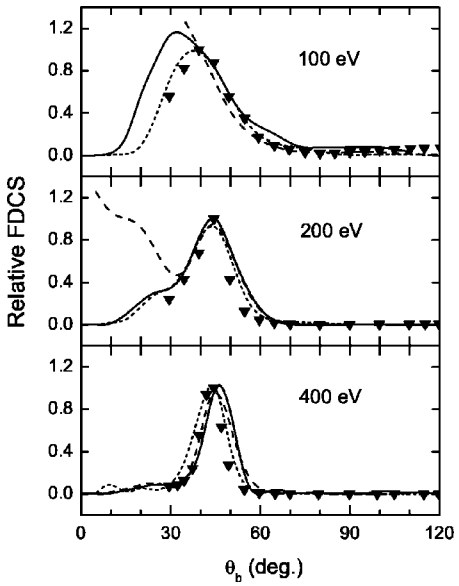


FIG. 2. Same as Fig. 1 except for higher incident-electron energies. Here the experimental data are those of Rioual *et al.* (Ref. 8).

## RESULTS

The process of interest is $e+N_2[(3\sigma_g)^2] \rightarrow 2e+N_2^+[(3\sigma_g)]$. Existing experiments have been performed in coplanar geometry for which the incident, scattered, and ejected electrons all lie in the scattering plane. Investigations have been performed in both coplanar symmetric and coplanar asymmetric geometries. In the coplanar symmetric case, the energy of each outgoing electron is $(E_i-E_0)/2$ eV where $E_0=15.6$ eV is the ionization energy of the $3\sigma_g$ state. Figure 1 compares the M3DW and DWBA with the coplanar symmetric experimental data of Hussey and Murray[9] for energies between 35.6 and 75.6 eV. Also shown in Fig. 1 are the DWIA results of Gao *et al.*[25] Except for 35.5 eV, the theoretical and relative experimental results are normalized to unity at the maximum experimental data point. For the 35.6 eV case the normalization was performed at 45°. The solid lines are the M3DW results, the longer dashed lines are the DWBA results, and the shorter dashed lines are the DWIA results.

From Fig. 1, it is seen that, of the three theories, the DWIA agrees best with the relative experimental data (i.e., the shape of the experimental data). The agreement with the experimental data gets better with increasing energy for both the M3DW and DWIA as one would expect for a first-order perturbation series calculation and by 75 eV, the DWIA is in very nice agreement with the experiment. Although the M3DW results are in qualitative agreement with the experiment, the M3DW consistently predicts a large angle peak that is not seen in the data, also the shape and location of the binary peak are not correct for 75 eV. There is very little resemblance between the DWBA model and the experimental data except perhaps for larger energies and angles. The DWBA does not even properly predict a binary peak at these low energies. For coplanar symmetric scattering, the cross section must vanish for 0° scattering when equal energy electrons are moving together in the beam direction. It is clear that the PCI term in the M3DW final-state wave function causes the 0° cross section to be zero whereas the first-order PCI in the DWBA is not sufficient to make the cross section vanish and the 0° DWBA cross section is unphysically large. Although the DWIA $T$ matrix does not contain PCI explicitly, it is interesting to note that the physics in the impulse approximation also causes the coplanar symmetric cross sections to vanish for 0° scattering.

Figure 2 compares coplanar symmetric DWIA, DWBA, and M3DW results with the experimental data of Rioual *et al.*[8] for incident-electron energies between 100 and 400 eV. Again, the theoretical and relative experimental results have been normalized to unity at the maximum in the experimental binary peak. It is seen that the agreement between the experiment and theory continues to improve with increasing incident-electron energy. The DWIA is in relatively good agreement with the experiment for the whole energy range and by 200 eV, the M3DW is also in relatively good agreement with the experiment. At 200 eV, the DWBA at least predicts a binary peak in agreement with the experiment and by 400 eV, all three theories are in reasonably good agreement with the experiment. The fact that DWBA and M3DW are almost the same at 400 eV indicates that the PCI has become unimportant by this energy for coplanar symmetric scattering. It is curious that the three theories predict slightly different locations for the binary peak at 400 eV and the DWIA is in the best agreement with the experiment for both the location and shape of the binary peak.

There is an important difference between the way the distorted waves are calculated for the present M3DW and the DWIA of Gao *et al.*[25] It is clear that polarization of the molecule by a continuum electron is likely to be important particularly for the lower-energy electrons. If the molecule is

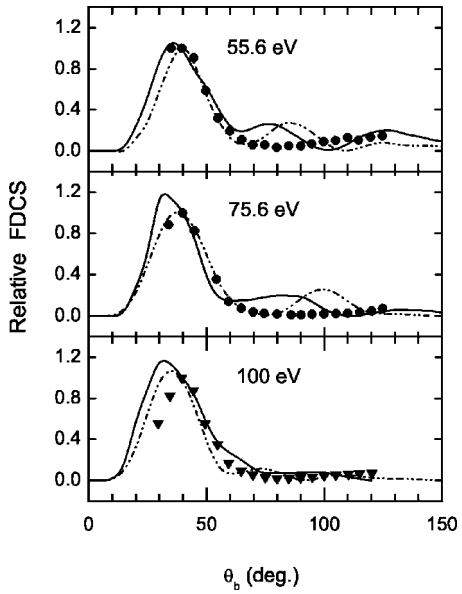


FIG. 3. Fully differential cross sections for electron-impact ionization of the $3\sigma_g$ state of $N_2$ for coplanar symmetric scattering. The energy of the incident electron is shown in each part of the figure and the horizontal axis is the angular location for the two electron detectors on the opposite sides of the beam direction. The solid lines are the M3DW results calculated without a polarization potential, the dashed double dotted lines are the M3DW results calculated with a polarization potential, the black circles are the experimental data of Hussey and Murray (Ref. 9), and the down triangles are the data of Rioual *et al.* (Ref. 8).

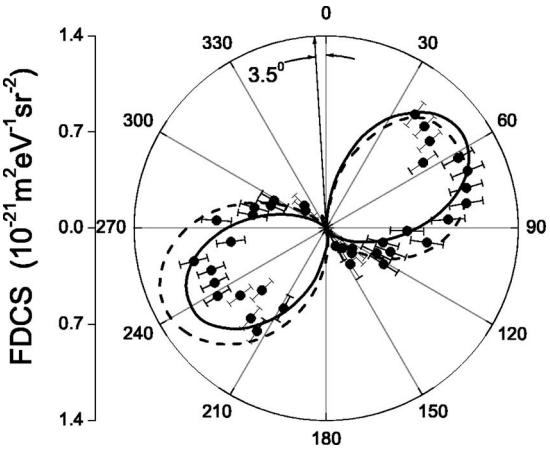


FIG. 4. Fully differential cross sections for electron-impact ionization of the $3\sigma_g$ state of $N_2$ for coplanar asymmetric scattering. The incident-electron energy is 295.6 eV and it is detected at a scattering angle $\theta_a$=3.5° measured counterclockwise relative to the beam direction, as indicated in the figure. The scattered electron has an energy of 270 eV and the ejected electron has an energy of 10 eV. The solid lines are the M3DW results, the dashed lines are the DWBA results, and the black circles are the experimental data of Avaldi *et al.* (Ref. 7). All the M3DW and DWBA results are normalized to the experimental data at $\theta_b$=68° in this figure.

polarized, this will affect the charge distribution and consequently the calculation of the distorted waves. Gao *et al.*[25] included the effect of polarization in the calculation of the distorted waves by using a phenomenological polarization potential with an adjustable cutoff radius and the radius was chosen to give the best fit of the DWIA to the experimental data. Since we do not like adjustable parameters (and were criticized for this procedure), we chose to not include polarization in the present calculations. However, it is nonetheless interesting to see the effect of this polarization potential.

In Fig. 3 we compare the M3DW results both with and without the polarization potential used by Gao *et al.*[25] for coplanar symmetric scattering with incident-electron energies between 55 and 100 eV. It is seen that the effect of the polarization potential is to shift the binary peak to higher angles and make the width more narrow which noticeably improves the agreement between the experiment and theory. Interestingly, the large angle peak at 55 and 75 eV shifts to larger angles but does not go away. At any rate, it appears that the lack of agreement between theory and the M3DW for energies above about 50 eV resulted not necessarily from a deficiency in the basic theoretical approach but rather from the omission of polarization in the calculation of the distorted waves. Although we do not feel like this is the best way to include polarization, it does appear that a M3DW with polarization properly included will probably be in good agreement with the experiment for energies around 50 eV and higher.

Figures 4–7 compare the present theoretical results with the coplanar asymmetric measurements of Avaldi *et al.*[7] The experimental measurements are absolute and we normalize the M3DW and DWBA results to the experimental data at 68° in Fig. 4 (we do not calculate absolute cross sections since we do not know all the necessary spectroscopic factors). On the other hand, since the experimental data are all absolute, only one normalization factor is used for all Figs. 4–7. Unlike the linear plots of Figs. 1–3, Figs. 4–7 are polar plots for which 0° is the incident-electron beam direction, the faster final-state electron is scattered to the left (counterclockwise) of the beam direction and the ejected electron is measured clockwise relative to the beam direction. The classical binary peak is the one to the upper right and the recoil peak is the one to the lower left. For Figs. 4 and 5, the incident-electron energy is 295.6 eV, the fast scattered-electron energy is 270 eV, and the slow ejected-electron energy is 10 eV. In Fig. 4, the fast electron is observed at a scattering angle of 3.5° and in Fig. 5 fast electron is observed at a scattering angle of 7.2°.

For Figs. 6 and 7, the incident-electron energy is 304 eV, the fast scattered-electron energy is 270 eV (same as Figs. 4

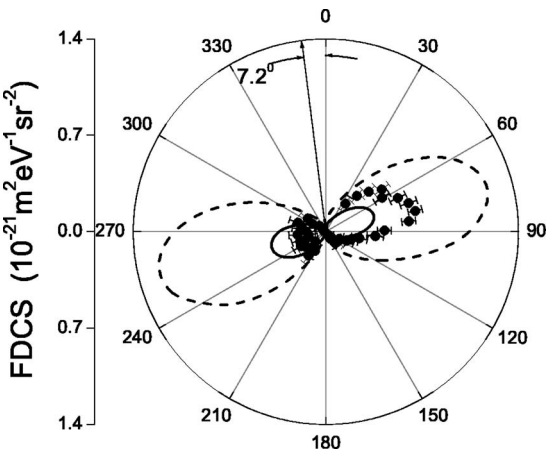


FIG. 5. Same as Fig. 4 except that the scattering angle $\theta_a$=7.2°.

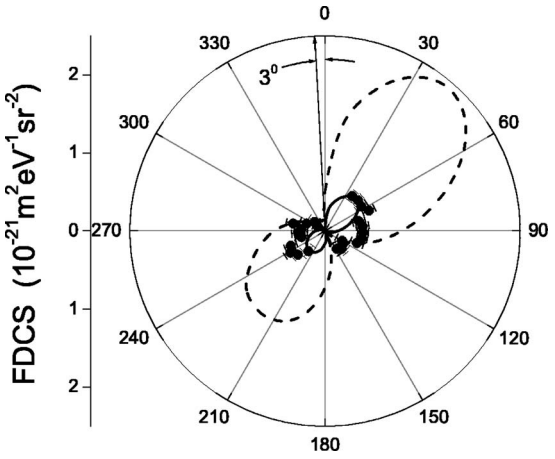


FIG. 6. Fully differential cross sections for electron-impact ionization of the $3\sigma_g$ state of $N_2$ for coplanar asymmetric scattering. The incident-electron energy is 304 eV and it is detected at a scattering angle $\theta_a$=3.0° measured counterclockwise relative to the beam direction, as indicated in the figure. The scattered electron has an energy of 270 eV and the ejected electron has an energy of 18.4 eV. The solid lines are the M3DW results, the dashed lines are the DWBA results, and the black circles are the experimental data of Avaldi *et al.* (Ref. 7).

and 5), and the slow ejected-electron energy is 18.4 eV. In Fig. 6 the fast electron is observed at a scattering angle of 3.0° and in Fig. 7 fast electron is observed at a scattering angle of 8.0°.

From Figs. 4–7 it is seen that the M3DW predicts the shape and relative magnitudes of the experimental data fairly well. In general, the binary peak is near the direction of the momentum transfer and the recoil peak is nearly opposite the momentum transfer. For the experimental data, Fig. 6 represents an exception to this rule in that both the binary and recoil peaks appear to be shifted to larger angles. We did not find a corresponding shift in the theoretical results and our binary peak is in the momentum-transfer direction. It is interesting to note that both the DWBA and M3DW predict about the same angular position for both the binary and recoil peaks for the different kinematical conditions. The DWBA, on the other hand, does not predict the relative magnitudes of the experimental data very well. Consequently, it is clear that the PCI is very important even for these highly asymmetric collisions and relatively high incident-electron energies. For the M3DW, the agreement with the experiment appears to be better for the smaller fast-electron scattering angles.

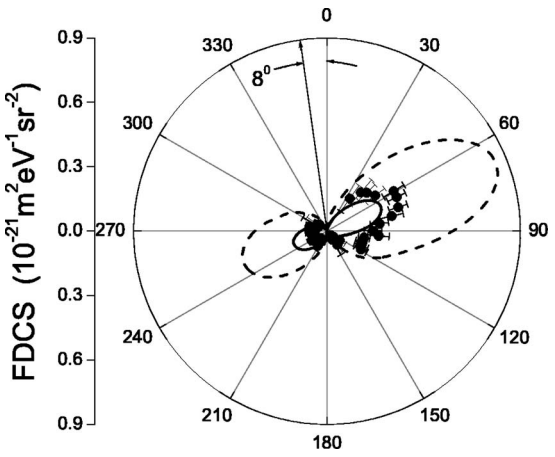


FIG. 7. Same as Fig. 6 except that the scattering $\theta_a$ equals 8.0°.

Although the DWBA is worse than M3DW for the coplanar asymmetry case, it is still much better than the DWIA (not shown) which has the wrong shape and incorrect peak positions. It is interesting that the DWIA works so well for the coplanar symmetric case but not the coplanar asymmetric case.

## CONCLUSION

We have calculated DWBA and M3DW FDCSs for the $e+N_2[(3\sigma_g)^2] \rightarrow 2e+N_2^+[(3\sigma_g)]$ process for both coplanar symmetric and coplanar asymmetric scatterings. In general, the M3DW results were significantly superior to the DWBA results. For coplanar symmetric scattering, experimental data were available down to 35.6 eV and the M3DW results were in qualitative agreement with the shape of the data for energies of 55.6 eV and above while the DWBA was not. In fact, the DWBA gave completely the wrong behavior for small scattering angles and low incident-electron energies. On the other hand, quantitative agreement between the M3DW and experiment for coplanar symmetric scattering was not achieved until about 200 eV. The DWIA calculated using a polarization potential was in reasonably good agreement with the experiment down to about 50 eV and, when polarization was added in the M3DW calculation, a reasonable agreement with the experiment was also achieved down to 50 eV. Consequently, these results indicate that the M3DW should be reliable for incident-electron energies of 50 eV and above if polarization of the molecule is taken into account in the calculation of the distorted waves.

For coplanar asymmetric scattering, the existing experimental data are for incident-electron energies in the vicinity of 300 eV and the data are absolute. The M3DW results were in fairly good agreement with both the shape and relative magnitudes of the measurements. While the DWBA shapes were similar to the data, the relative magnitudes were wrong. Since the difference between the DWBA and M3DW lies only in the treatment of the PCI (M3DW contains the PCI to all orders of perturbation theory while DWBA treats the PCI only to first order), it is clear that the PCI is very important for both coplanar symmetric scattering and coplanar asymmetric scattering even for energies as high as 300 eV. In fact, contrary to intuition, it appears that the PCI may be even more important for coplanar asymmetric scattering than for symmetric scattering since the DWBA and the M3DW results were almost the same for the 400 eV symmetric scattering case while large differences were found in the 300 eV asymmetric scattering case. The DWIA gives completely incorrect results for the coplanar asymmetric case considered here.

[1] I. E. McCarthy and E. Weigold, Phys. Rep. C **27**, 275 (1976).
[2] I. E. McCarthy and E. Weigold, Rep. Prog. Phys. **51**, 299 (1988).
[3] I. E. McCarthy and A. M. Rossi, Phys. Rev. A **49**, 4645 (1994).
[4] E. Weigold and I. E. McCarthy, *Electron Momentum Spectroscopy* (Kluwer, Dordrecht/Plenum, New York, 1999).
[5] K. T. Leung and C. E. Brion, J. Electron Spectrosc. Relat. Phenom. **35**, 327 (1985).

[6] K. Jung, E. Schubert, D. A. L. Paul, and H. Ehrhardt, J. Phys. B **8**, 1330 (1975).
[7] L. Avaldi, R. Camilloni, E. Fainelli, and G. Stefani, J. Phys. B **25**, 3551 (1992).
[8] S. Rioual, G. N. Vien, and A. Pochat, Phys. Rev. A **54**, 4968 (1996).
[9] M. J. Hussey and A. Murray, J. Phys. B **35**, 3399 (2002).
[10] A. J. Murray, J. Phys. B **38**, 1999 (2005).
[11] M. J. Hussey and A. J. Murray, J. Phys. B **38**, 2965 (2005).
[12] D. S. Milne-Brownlie, S. J. Cavanagh, B. Lohmann, C. Champion, P. A. Hervieus, and J. Hanssen, Phys. Rev. A **69**, 032701 (2004).
[13] A. Lahmam-Bennani, I. Taouil, A. Duguet, M. Lecas, L. Avaldi, and J. Berakdar, Phys. Rev. A **59**, 3548 (1999).
[14] I. Taouil, A. Lahmam-Bennani, A. Duguet, and L. Avaldi, Phys. Rev. Lett. **81**, 4600 (1998).
[15] M. Chérid, A. Lahmam-Bennani, A. Duguet, R. W. Zurales, R. R. Lucchese, M. C. Dal Cappello, and C. Dal Cappello, J. Phys. B **22**, 3483 (1989).
[16] F. Robicheaux, J. Phys. B **29**, 779 (1996).
[17] H. Deutch and K. Becker, J. Phys. Chem. A **102**, 8819 (1998).
[18] C. Champion, J. Hanssen, and P. A. Hervieux, Phys. Rev. A **63**, 052720 (2001).
[19] A. L. Monzani, L. E. Machado, M. T. Lee, and A. M. Machado, Phys. Rev. A **60**, R21 (1999).
[20] P. Weck, O. A. Fojon, J. Hannsen, B. Joulakian, and R. D. Rivarola, Phys. Rev. A **63**, 042709 (2001).
[21] C. R. Stia, O. A. Fojón, P. F. Weck, J. Hanssen, B. Joulakian, and R. D. Rivarola, Phys. Rev. A **66**, 052709 (2002).
[22] J. Gao, D. H. Madison, and J. L. Peacher, Phys. Rev. A **72**, 020701(R) (2005).
[23] J. Gao, J. L. Peacher, and D. H. Madison, AIP Conf. Proc. (to be published).
[24] J. Gao, D. H. Madison, and J. L. Peacher, J. Chem. Phys. (to be published).
[25] J. Gao, D. H. Madison, and J. L. Peacher, Phys. Rev. A **72**, 032721 (2005).
[26] M. W. Schmidt, K. K. Baldridge, J. A. Boats *et al.*, J. Comput. Chem. **14**, 1347 (1993).
[27] A. Prideaux and D. H. Madison, J. Phys. B **37**, 4423 (2004).
[28] A. Prideaux, D. H. Madison, and K. Bartschat, Phys. Rev. A **72**, 032702 (2005).
[29] M. A. Haynes, B. Lohmann, A. Prideaux, and D. H. Madison, J. Phys. B **36**, 811 (2003).
[30] M. Brauner, J. S. Briggs, and H. Klar, J. Phys. B **22**, 2265 (1989).
[31] J. B. Furness and I. E. McCarthy, J. Phys. B **6**, 2280 (1973).
[32] A. Prideaux and D. H. Madison, Phys. Rev. A **67**, 052710 (2003).